

Band-Edge Noise Spectroscopy of a Magnetic Tunnel Junction

Farkhad G. Aliev* and Juan Pedro Cascales

Departamento Física de la Materia Condensada C-III, Instituto Nicolas Cabrera (INC) and Condensed Matter Physics Institute (IFIMAC), Universidad Autonoma de Madrid, Madrid 28049, Spain

Ali Hallal and Mairbek Chshiev

*Université Grenoble Alpes, INAC-SPINTEC, F-38000 Grenoble, France;
CEA, INAC-SPINTEC, F-38000 Grenoble, France; and
CNRS, SPINTEC, F-38000 Grenoble, France*

Stephane Andrieu

Institut Jean Lamour, UMR CNRS 7198, Université de Lorraine, F-54506 Nancy, France

(Received 15 January 2014; revised manuscript received 8 May 2014; published 27 May 2014)

We propose a conceptually new way to gather information on the electron bands of buried metal-(semiconductor-)insulator interfaces. The bias dependence of low frequency noise in $\text{Fe}_{1-x}\text{V}_x/\text{MgO}/\text{Fe}$ ($0 < x < 0.25$) tunnel junctions shows clear anomalies at specific applied voltages, reflecting electron tunneling to the band edges of the magnetic electrodes. The change in magnitude of these noise anomalies with the magnetic state allows evaluating the degree of spin mixing between the spin polarized bands at the ferromagnet-insulator interface. Our results are in qualitative agreement with numerical calculations.

DOI: 10.1103/PhysRevLett.112.216801

PACS numbers: 73.20.At, 72.70.+m, 73.22.-f, 73.40.Gk

Buried metal-(semiconductor-)insulator interfaces are found at the heart of electronics [1]. The current in tunneling devices is determined by the bias, barrier, and density of states of the electrodes [2,3]. Electron states not allowed in bulk could become permitted at the surface leading to topological [4,5] or interface resonant states [6]. For metallic structures the scarce knowledge on the interface bands is mainly obtained by indirect methods such as ballistic electron emission spectroscopy [7] or high-resolution x-ray photoelectron spectroscopy [8]. The possibility of reliable and down-scalable *in situ* methods to investigate interface electron bands remains centrally important [9].

Tunneling magnetoresistance [10–12] is extremely sensitive to the band structures of ferromagnet-insulator (FM/I) interfaces [3,13–20]. Despite recent attempts to understand the nature of the electron bands which contribute to electron transport in spintronic devices [21–23], the issue remains unsettled. The main tool to characterize interfaces or barriers has been inelastic electron tunneling spectroscopy (IETS) [23–25], analyzing the derivative of the conductance as a function of bias. The resulting IETS signals depend on the tunneling density of states (DOS) and inelastic scattering [2,3,26], which could obscure the detection of the band edges in the presence of interface disorder. The bias dependence of the conductance and its low frequency fluctuations could be an alternative way to study the interface or electron confinement [27,28] DOS.

A commonly accepted phenomenological approach relates the excess low frequency noise (LFN), often inversely dependent on the frequency f , with electrons

scattering from defects characterized by a broad distribution of relaxation times with energy [29]. If dominant defect states are located close to the interfaces, they could create interface band edge tails [see Supplemental Material Fig. 1(a) or Fig. S.1(a) [30]]. Therefore, when the tunneling is tuned to some specific band edge in the opposite electrode, the current could acquire an extra LFN due to multiple relaxations originating from defect states contributing to the formation of the band edge tails [Fig. S.1(b) [30]].

In this Letter we investigate the bias dependence of conductance and LFN in single barrier tunneling devices in order to determine *in situ* the energies of the band edges of the buried interfaces. We unambiguously demonstrate the validity of the band edge noise spectroscopy (BENS) concept by studying seminal $\text{Fe}/\text{MgO}/\text{Fe}$ magnetic tunnel junctions (MTJs) with partial doping of the bottom electrode (Fe) with Vanadium (V). Such substitution has been shown to reduce defect states inside the MgO barrier due to improved interface matching between $\text{Fe}_{1-x}\text{V}_x$ and MgO in $\text{Fe}_{1-x}\text{V}_x/\text{MgO}/\text{Fe}$ MTJs [31–33]. Our numerical simulations confirm that tunneling of band-tail electrons, influenced by spin-orbit interactions, are responsible for the observed LFN anomalies.

Our magnetic tunnel junctions were grown by molecular beam epitaxy on MgO (100) substrates under ultrahigh vacuum (typically 10^{-10} mbar) conditions. Fe-V alloys were grown at room temperature by coevaporation, the layer being afterwards annealed up to 900 K. The barrier thickness was controlled by RHEED intensity oscillations. The MTJs were patterned by UV photolithography and Ar

etching to dimensions ranging from 10 to 50 μm . More details can be found in [31]. The noise measurements setup was described earlier [34,35]. The typical noise power spectra (S_V) in the antiparallel (AP) or parallel (P) states reveal the presence of $1/f$ noise in the frequency range between 1 and 50 Hz as $S_V(f) \propto 1/f^\beta$ [with $0.8 < \beta < 1.5$, see Fig. S.1(b) in [30]]. The bias dependence of the LFN has been determined through the Hooge factor (α) from the phenomenological expression: $S_V(f) = \alpha(I \cdot R)^2 / (A f)$, where R , I , A , and f indicate resistance, current, area, and frequency, respectively [35]. Qualitatively similar results have been obtained by analyzing integrated LFN [Fig. S.1(c) [30]]. Shot noise (SN) was obtained from the frequency independent part of the LFN below 10 K [34].

We begin by analyzing the electron transport and SN behavior at $T = 4$ K. The zero bias tunneling magnetoresistance (TMR) as a function of V content shows a maximum [Fig. 1(a)], confirming a reduction of the interface mismatch reported previously at room temperature [31–33]. The nearly Poissonian character of the tunneling statistics with Fano factor $F = 1 \pm 0.05$ [Fig. 1(a)] indicates nearly direct tunneling processes.

Figure 1(b) shows the bias dependence of the Hooge factor $\alpha(V)$ in both P and AP states for a Fe/MgO/Fe MTJ used as reference. One observes an excess LFN below 200 mV, where FeO [36] and Fe/MgO [2] interface defect states have been predicted to influence the conductance.

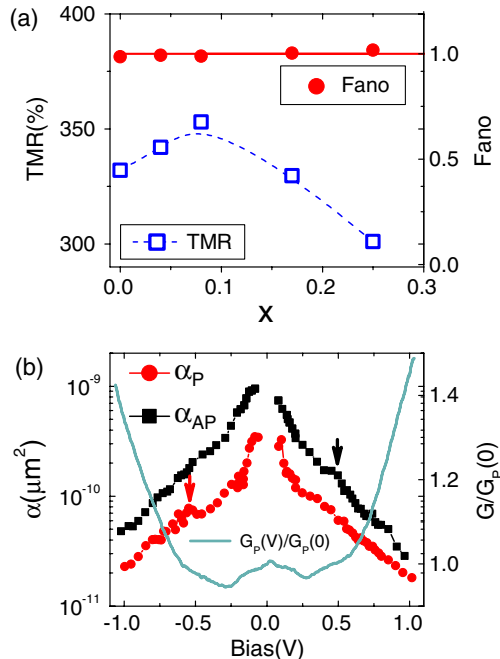


FIG. 1 (color online). (a) Dependence of the zero bias TMR and the Fano factor at $T = 4$ K as a function of V content. (b) Bias dependence, at $T = 4$ K, of the dynamic conductance in the P state, and the Hooge factor α of both P and AP states for Fe/MgO/Fe junctions. Arrows indicate weak peaks.

For the MTJ with a nonoptimized Fe/MgO interface one observes a strong suppression of LFN with bias with weak anomalies in the $\alpha(V)$ around 0.5 V, indicated by arrows.

The doping of Fe with V improves the interface mismatch and decreases the Fe/MgO interface defect states density [31–33], which allows the implementation of the BENS method. Figure 2(a) shows the $\alpha(V)$ and SN(V) dependence for $\text{Fe}_{0.96}\text{V}_{0.04}/\text{MgO}/\text{Fe}$ MTJs. The SN(V) gives a Fano factor close to one, proving direct tunneling in the bias range under study [Fig. 2(a)]. In contrast to what is observed for the reference sample (Fig. 1), the LFN shows a clear enhancement (factor of 2) of conductance fluctuations around ± 0.6 V. Yet a stronger enhancement of the LFN close to 0.6 V is observed in the AP configuration. The dynamic conductance in both states shows an upturn around 0.6 V, but appears clearer in the P state [Fig. 2(b), AP state not shown for simplicity]. Numerical calculations of the tunneling electron DOS indicate that the upturn in conductance and the noise enhancement could be related with the opening of a new transmission channel when the Fermi level of one magnetic electrode crosses one of the band edges of the other magnetic electrode, indicated by arrows in Fig. 2(b).

Even clearer signs of the band edges in LFN are seen with an 8% of V where the lowest background LFN and the maximum TMR (Fig. 1) are achieved. Figure 3 shows $\alpha(V)$

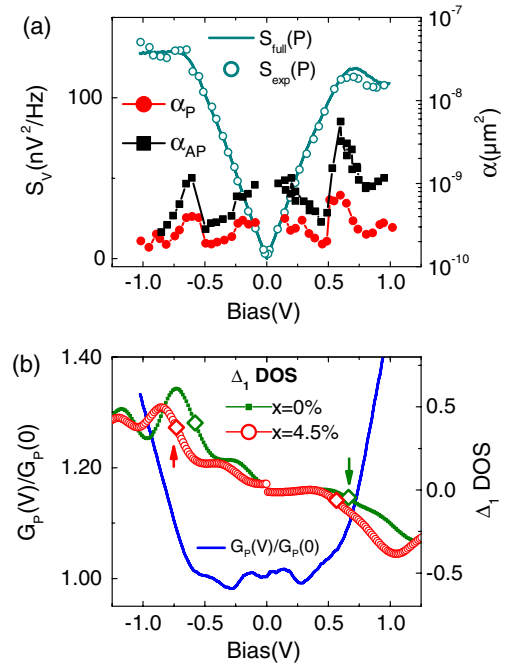


FIG. 2 (color online). (a) Bias dependence at $T = 4$ K of the Hooge factor and SN for $\text{Fe}_{0.96}\text{V}_{0.04}/\text{MgO}/\text{Fe}$ MTJ. (b) Dependence of the conductance with the applied voltage at $T = 4$ K combined with the calculated Δ_1 DOS as a function of energy with respect to E_F . Inflection points (open dots) indicate Δ_1 DOS band edges for 4% vanadium for $V < 0$ and pure Fe ($x = 0$) for $V > 0$.

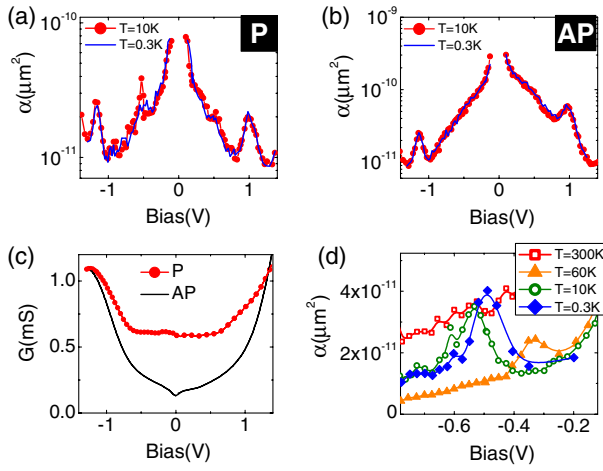


FIG. 3 (color online). Bias dependence at $T = 4$ K of the Hooke coefficient for the (a) P state and (b) AP state in $\text{Fe}_{0.92}\text{V}_{0.08}/\text{MgO}/\text{Fe}$ MTJs. (c) Bias dependence at $T = 4$ K of the dynamic conductance for the P and AP state. (d) Low frequency noise peaks gradually disappear with increasing temperature.

dependence in $\text{Fe}_{0.92}\text{V}_{0.08}/\text{MgO}/\text{Fe}$ MTJs were the optimum relation between two competing effects is reached: FM/I interface relaxation on the one side and still not essential suppression of the magnetization and the induced Fe-V structural disorder on the other side [31–33]. We estimate the TMR from our simulations using the Jullière model [10] (Fig. S.2 [30]) which indicates the optimum values are reached for 9% of V, i.e., rather close to what is experimentally observed. We have found that the $\text{Fe}_{0.92}\text{V}_{0.08}/\text{MgO}/\text{Fe}$ MTJs show clear anomalies in the Hooke factor for biases around 1 V and around 0.6 V for the P state only, as shown in Figs. 3(a) and 3(b). Figure 3(d) demonstrates how the anomaly in the P state around 0.6 V gradually disappears with temperature, probably due to thermal excitations.

Qualitatively similar effects were seen for $\text{Fe}_{0.83}\text{V}_{0.17}/\text{MgO}/\text{Fe}$ and $\text{Fe}_{0.75}\text{V}_{0.25}/\text{MgO}/\text{Fe}$ MTJs with the latter being the most robust to electrical breakdown (standing up to 2.5 V). In the high V content range, the LFN is strongly influenced by random telegraph noise at positive biases around 1 V, reflecting a strongest asymmetry in interface defect states previously visualized with scanning electron microscopy for $\text{Fe}_{0.8}\text{V}_{0.2}/\text{MgO}/\text{Fe}$ MTJs [33].

Figure 4(a) qualitatively explains the BENS method. As long as tunneling through the barrier is coherent, the main source for LFN are conductance fluctuations due to atomic defects affecting Δ_1 and Δ_5 interface states. Resulting localized states close to the band edges [37] could contribute, as reported for bulk semiconductors [38,39], to the enhanced LFN. The key new feature of the BENS is the versatility in displacing the Fermi level [E_F in Fig. 4(a)] of the ejector electrode with respect to the different band edges [or mobility edge, E_C in Fig. 4(a)] by simply varying the

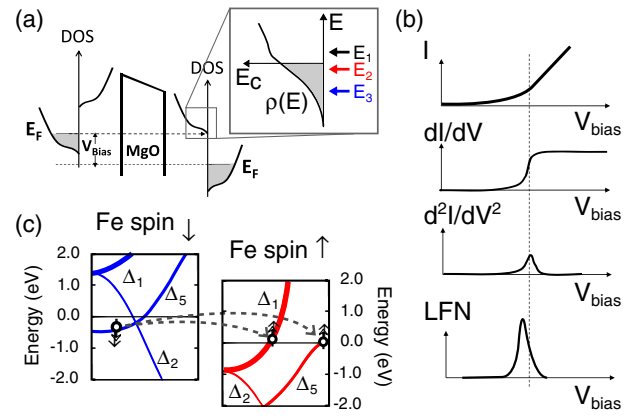


FIG. 4 (color online). (a) Sketch of the principle behind BENS, presented for the AP state, where E_C corresponds to the mobility edge. (b) The energies of these defect states can be inferred from the I - V curve of the sample, and its first (dynamic conductance) and second (IETS) derivatives, but they are detected in a much clearer way though low frequency measurements. (c) Sketch of a band edge (Δ_1 , Δ_5) contribution to the tunneling at ~ -1.2 V.

applied bias. The right panel shows how the conductance and its derivatives are expected to change when a new electron channel with a band edge opens at E_F . In order to clearly detect inelastic relaxation through IETS, some well-defined defect states should relax energy through coupling to a well-defined set of phonon energies. We believe that the random interface potential and the absence of well-defined defect states smear out the IETS signals. Tunneling to the band tail weakly influences IETS [inset of Fig. S.1(c) [30]] reflecting only the derivative of the DOS close to E_C . On the other hand, much stronger changes in LFN vs bias are seen due to a strong change of excited defect relaxation times [39] when tunneling close to E_C , activating an excess of the low frequency conductance fluctuations. Therefore, interface defect states dominate the LFN, and not the derivative of the conductance [inset of Fig. S.1(c) [30]].

The following arguments indicate that LFN mainly originates from disorder or defects close to the FM/I interface: (i) direct tunneling (Fig. 1); (ii) the metallic nature of the electrodes, with resistance a few thousand times below the barrier resistance, ensuring that electric signals and their fluctuations mainly come from regions in the barrier and interfaces; (iii) by analyzing LFN at higher biases we avoid direct resonant excitation of localized FeO or O interface defect levels predicted below 200 mV [36].

A simplified physical picture explaining the variation of LFN when tunneling to three different energies $E_{1,2,3}$ around E_C [Fig. 4(a) and Fig. S.1 [30]] is as follows. When electrons tunnel to energies $E_1 > E_C$, their relaxation time is fast due to the delocalized character of the band states near E_1 with a correspondingly small contribution to LFN. For tunneling to electron states $E_3 < E_C$ the LFN is also expected to be small due to the low probability of these tunneling events. However, when electrons tunnel to the

energies $E_2 \lesssim E_C$, the tunneling current could be affected by multiple trapping-type relaxations originating from shallow defect states contributing to the formation of the band edge tails. We estimate that the LFN peak width is roughly determined by the energy difference between the mobility edge and the bottom of the band tail.

In the MTJs under study, electron tunneling mainly occurs between polarized bands with different Bloch state $\Delta_{1,5}$ symmetries spin filtered by the MgO barrier [14–19]. This allows a rough estimation of the interband mixing at the interface by analyzing a variation of the BENS response with relative alignment of the electrodes. Let us discuss qualitatively the reasons why BENS could provide LFN peaks both in the P and AP states (Figs. 2, 3). For simplicity, we shall use the majority and minority Fe electron bands tunneling in Fe/MgO/Fe junctions [Fig. 4(c)]. When the MTJ is in the AP state, then in accordance with BENS arguments $\Delta_{5\uparrow} \Rightarrow \Delta_{5\downarrow}$ and $\Delta_{1\uparrow} \Rightarrow \Delta_{1\downarrow}$ band edge tunneling could provide a peak in LFN (AP) at different biases from 0.4 to 1.3 V if conductance fluctuations originate from elastic scattering events. Experimentally, however, we observe LFN peaks in the P state too [Fig. 2(a)], which we link with the presence of spin-orbit coupling induced $\Delta_{1(\uparrow\downarrow)} \Leftrightarrow \Delta_{5(\downarrow\uparrow)}$ interband mixing at the Fe/MgO interface [40]. Indeed, large lateral momentum transfer and interband scattering could be dominant only close to the interfaces [41]. Within such a scenario, the relation between amplitudes of the peaks LFN(P)/LFN(AP) provides an evaluation of the degree of interband mixing between the majority $\Delta_{1\uparrow}$ band and the minority $\Delta_{5\downarrow}$ of roughly 0.2–0.3.

In order to examine quantitatively the applicability of our model we have performed *ab initio* calculations of a $\sqrt{2} \times \sqrt{2}$ unit cell of $\text{Fe}_{1-x}\text{V}_x/\text{MgO}$ ($x = 0, 0.045, 0.091, 0.182$) with a 5 monolayers (ML) of MgO and 11 ML of $\text{Fe}_{1-x}\text{V}_x$. Our first-principles calculations are based on density functional theory as implemented in the Vienna *ab initio* simulation package (VASP) [42] within the framework of the projector augmented wave potentials [43] to describe electron-ion interaction and generalized gradient approximation [44] for exchange-correlation interactions. A $13 \times 13 \times 3$ K -point mesh was used in our calculations. A plane wave energy cutoff equal to 500 eV for all calculations was used and is found to be sufficient for our system.

Figure 5 compares the experimentally observed LFN anomalies in the P state (open dots) with the band edge positions (closed dots) estimated from inflection points in the DOS simulations for the majority and minority Δ_1 and Δ_5 states of $\text{Fe}_{1-x}\text{V}_x/\text{MgO}$ ($x = 0, 0.045, 0.091, 0.182$) structures [as indicated by arrows in Fig. 2(b)]. We have also indicated by horizontal dotted lines the estimated positions of the band edges of the Fe/MgO structure.

A reasonable agreement between simulation and experiment is observed, especially for the vanadium content

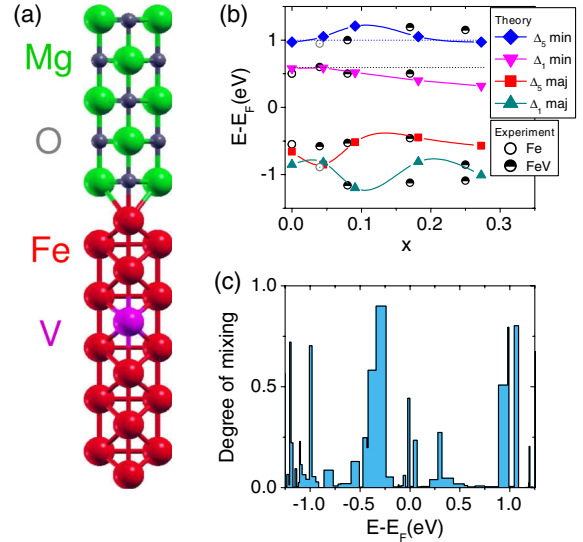


FIG. 5 (color online). (a) Schematic of the calculated crystalline structure for a $\sqrt{2} \times \sqrt{2}$ unit cell of $(\text{Fe}_{1-x}\text{V}_x)_{11}/\text{MgO}_5$. (b) Calculated changes in the energies of the band edges in $\text{Fe}_{1-x}\text{V}_x$ compared to the experimental data of low frequency noise anomalies for the P state. Fully open experimental points indicate a weak peak (increase of noise in less than 10%). (c) Calculated degree of mixing between Δ_1 and Δ_5 interface Bloch state character in $(\text{Fe}_{1-x}\text{V}_x)_1/\text{MgO}_5$ for $x = 0.091$.

between ($0.04 < x < 0.17$) with reduced lattice mismatch, the lowest background LFN and the highest TMR.

A few factors could contribute to some difference between experimental results and calculations. First of all, calculations do not consider the presence of dislocation induced mismatch as well as the structural disorder difference between bottom and top interfaces [33]. On the experimental side, measurements on MTJs with the least vanadium were done below 1 V due to their vulnerability, making them difficult to compare with the calculation results above 1 V.

Finally, in order to better understand the influence of spin mixing at the interface, we have also analyzed the Bloch state character of the interfacial Fe atom in the presence of SOI as a function of the energy difference to E_F . Figure 5(c) presents this analysis for Δ_1 and Δ_5 interface states in $\text{Fe}_{0.909}\text{V}_{0.091}/\text{MgO}$ structure, mainly participating in the electron tunneling through MgO. When the degree of mixing at certain energy is equal to zero, it means that there is no mixing between different Δ channels and there is only one Δ Bloch state character that dominates the tunneling at this energy tunneling. The channel mixing is more pronounced at biases around $-(0.4-0.5)$ V and not above ± 1 V, i.e., close to the intervals where LFN anomalies of different magnitude were observed in both magnetic states [Fig. 5(c)]. We believe that $\Delta_{5\uparrow} \Rightarrow \Delta_{5\downarrow}$ and $\Delta_{1\uparrow} \Rightarrow \Delta_{5\downarrow}$ mixing could be due to surface induced band crossings and explains the appearance of peaks in LFN both in the P and AP states.

To summarize, we have introduced the band edge noise spectroscopy concept which permits an investigation of the electron band edges in a wide class of tunneling devices. We demonstrated successfully BENS approach in epitaxial magnetic tunnel junctions. The dependence of the BENS on the relative magnetic alignment of the electrodes allows us to estimate the importance of interband hybridization and spin flips at the FM/I interfaces. Given the crucial importance of buried interfaces in solid-state devices, the clear need to understand their electronic structure, and the limited options available, our work presents a substantial advance in the field of characterizing buried interfaces.

The authors acknowledge A. Gomez-Ibarlucea, D. Herranz, and F. Bonell for their help with the experiments and sample growth. This work has been supported by the Spanish MINECO (MAT2012-32743) and Comunidad de Madrid (P2009/MAT-1726) Grants.

*Corresponding author.
farkhad.aliev@uam.es

- [1] H. Kroemer, *Rev. Mod. Phys.* **73**, 783 (2001).
- [2] C. Tiusan, F. Greullet, M. Hehn, F. Montaigne, S. Andrieu, and A. Schuhl, *J. Phys. Condens. Matter* **19**, 165201 (2007).
- [3] S. Yuasa and D. D. Djayaprawira, *J. Phys. D* **40**, R337 (2007).
- [4] M. Z. Hasan and C. L. Kane, *Rev. Mod. Phys.* **82**, 3045 (2010).
- [5] T. Schlenk *et al.*, *Phys. Rev. Lett.* **110**, 126804 (2013).
- [6] K. D. Belashchenko, J. Velev, and E. Y. Tsymlal, *Phys. Rev. B* **72**, 140404R (2005).
- [7] L. D. Bell and W. J. Kaiser, *Phys. Rev. Lett.* **61**, 2368 (1988).
- [8] F. Bonell *et al.*, *Phys. Rev. Lett.* **108**, 176602 (2012).
- [9] R. F. Berger, C. J. Fennie, and J. B. Neaton, *Phys. Rev. Lett.* **107**, 146804 (2011).
- [10] M. Jullière, *Phys. Lett.* **54A**, 225 (1975).
- [11] J. S. Moodera, L. R. Kinder, T. M. Wong, and R. Meservey, *Phys. Rev. Lett.* **74**, 3273 (1995).
- [12] T. Miyazaki and N. Tezuka, *J. Magn. Magn. Mater.* **139**, L231 (1995).
- [13] J. M. De Teresa *et al.*, *Science* **286**, 507 (1999).
- [14] W. H. Butler, X.-G. Zhang, T. C. Schulthess, and J. M. MacLaren, *Phys. Rev. B* **63**, 054416 (2001).
- [15] J. Mathon and A. Umerski, *Phys. Rev. B* **63**, 220403(R) (2001).
- [16] M. Bowen *et al.*, *Appl. Phys. Lett.* **79**, 1655 (2001).
- [17] J. Faure-Vincent, C. Tiusan, E. Jouguelet, F. Canet, M. Sajieddine, C. Bellouard, E. Popova, M. Hehn, F. Montaigne, and A. Schuhl, *Appl. Phys. Lett.* **82**, 4507 (2003).
- [18] S. S. P. Parkin, C. Kaiser, A. Panchula, P. M. Rice, B. Hughes, M. Samant, and S.-H. Yang, *Nat. Mater.* **3**, 862 (2004).
- [19] S. Yuasa, T. Nagahama, A. Fukushima, Y. Suzuki, and K. Ando, *Nat. Mater.* **3**, 868 (2004).
- [20] D. A. Stewart, *Nano Lett.* **10**, 263 (2010).
- [21] P.-J. Zermatten, G. Gaudin, G. Maris, M. Miron, A. Schuhl, C. Tiusan, F. Greullet, and M. Hehn, *Phys. Rev. B* **78**, 033301 (2008).
- [22] I. Rungger, O. Mryasov, and S. Sanvito, *Phys. Rev. B* **79**, 094414 (2009).
- [23] T. Harada, I. Ohkubo, M. Lippmaa, Y. Sakurai, Y. Matsumoto, S. Muto, H. Koinuma, and M. Oshima, *Phys. Rev. Lett.* **109**, 076602 (2012).
- [24] R. C. Jaklevic and J. Lambe, *Phys. Rev. Lett.* **17**, 1139 (1966).
- [25] J. M. Teixeira, J. Ventura, J. P. Araujo, J. B. Sousa, P. Wisniowski, S. Cardoso, and P. P. Freitas., *Phys. Rev. Lett.* **106**, 196601 (2011).
- [26] D. Wortmann, H. Ishida, and S. Blügel, *Phys. Rev. B* **72**, 235113 (2005).
- [27] K. Nikolic and A. MacKinnon, *Phys. Rev. B* **50**, 11008 (1994).
- [28] G. Xu, C. M. Torres, E. B. Song, J. Tang, J. Bai, X. Duan, Y. Zhang, and K. L. Wang, *Nano Lett.* **10**, 4590 (2010).
- [29] P. Dutta and P. M. Horn, *Rev. Mod. Phys.* **53**, 497 (1981).
- [30] See Supplemental Material at <http://link.aps.org/supplemental/10.1103/PhysRevLett.112.216801> for $1/f$ phenomenological model, band-edge detection and details of numerical calculations.
- [31] F. Bonell *et al.*, *IEEE Trans. Magn.* **45**, 3467 (2009).
- [32] D. Herranz, F. Bonell, A. Gomez-Ibarlucea, S. Andrieu, F. Montaigne, R. Villar, C. Tiusan, and F. G. Aliev, *Appl. Phys. Lett.* **96**, 202501 (2010).
- [33] F. Bonell, S. Andrieu, C. Tiusan, F. Montaigne, E. Snoeck, B. Belhadji, L. Calmels, F. Bertran, P. Le Fèvre, and A. Taleb-Ibrahimi, *Phys. Rev. B* **82**, 092405 (2010).
- [34] R. Guerrero, F. G. Aliev, Y. Tserkovnyak, T. S. Santos, and J. S. Moodera, *Phys. Rev. Lett.* **97**, 266602 (2006).
- [35] R. Guerrero, D. Herranz, F. G. Aliev, F. Greullet, C. Tiusan, M. Hehn, and F. Montaigne, *Appl. Phys. Lett.* **91**, 132504 (2007).
- [36] G. X. Du, S. G. Wang, Q. L. Ma, Y. Wang, R. C. C. Ward, X.-G. Zhang, C. Wang, A. Kohn, and X. F. Han, *Phys. Rev. B* **81**, 064438 (2010).
- [37] S. Fahy, A. Lindsay, H. Ouerdane, and E. P. O'Reilly, *Phys. Rev. B* **74**, 035203 (2006).
- [38] R. Jayaraman and C. G. Sadini, *IEEE Trans. Electron Devices* **36**, 1773 (1989).
- [39] E. Borovitskaya and M. S. Shur, *Solid State Electron.* **45**, 1067 (2001).
- [40] Y. Lu *et al.*, *Phys. Rev. B* **86**, 184420 (2012).
- [41] *Handbook on Spin Transport and Magnetism*, edited by E. Y. Tsymlal and I. Zutic (Chapman and Hall/CRC, London, 2012), p. 246.
- [42] G. Kresse and J. Hafner, *Phys. Rev. B* **47**, 558 (1993); G. Kresse and J. Furthmüller, *Phys. Rev. B* **54**, 11 169 (1996); *Comput. Mater. Sci.* **6**, 15 (1996).
- [43] P. E. Blöchl, *Phys. Rev. B* **50**, 17 953 (1994); G. Kresse and D. Joubert, *Phys. Rev. B* **59**, 1758 (1999).
- [44] Y. Wang and J. P. Perdew, *Phys. Rev. B* **44**, 13 298 (1991).